PHYSICAL REVIEW D VOLUME 45, NUMBER 11 1 JUNE 1992

Finite-temperature QCD sum rules for the nucleon

C. Adami and I. Zahed
Physics Department, State University of New York at Stony Brook, Stony Brook, New York 11794
(Received 11 July 1991)

Using the QCD sum rules, we investigate the effects of temperature on the nucleon below the phase transition. The mass and width of the nucleon are analyzed using various parametrizations of the nucleon continuum. Overall, the nucleon mass is found to depend substantially on temperature variations in the quark condensate, irrespective of the continuum parametrization. Our results are compared with the ones discussed in the context of the chiral approach.

PACS number(s): 11.50.Li, 12.38.Mh, 14.20.Dh

I. INTRODUCTION

Considerable attention has been paid recently to the properties of nuclear matter under extreme conditions. The general consensus seems to be that nuclear matter undergoes a phase transition from a strongly confined phase of hadrons at low temperature to a weakly interacting phase of quarks and gluons at high temperature. The evidence for such behavior comes mainly from lattice simulations [1], and more recently from chiral perturbation theory in the low-temperature approximation [2–4]. The high-temperature phase is believed to be nonperturbative because of persisting infrared problems.

In a recent paper [5] we have critically analyzed the use of finite-temperature QCD sum rules. In particular, we have found that the ρ-meson mass and width varied slowly at low temperature. A rapid variation in the ρ-meson parameters was noted near T_c, following primarily large variations in the quark condensate. At these temperatures, however, the QCD sum-rule procedure was shown to break down. This notwithstanding, the analysis proved to be an interesting tool for investigating low-temperature effects on real-time correlation functions in the timelike regime. Needless to say, these correlation functions are not accessible to present-day Euclidean lattice formulations.

In this paper we pursue our investigation of the low-temperature effects on the nucleon parameters, following the analysis outlined in [5]. This is particularly interesting in light of recent and future relativistic heavy-ion experiments that attempt to create conditions of high density and temperature in the laboratory. Since heavy ions are predominantly composed of nucleons, we expect that possible structural changes in the nucleon properties following local thermalization or compression should be amenable to a QCD description. We note that variations in the hadronic masses might shed some light upon the nature of a possible QCD phase transition, and be of some relevance for nucleosynthesis scenarios in the early Universe [6].

In Sec. II we briefly review the QCD sum-rule technique at zero temperature in the nucleon channel. This construction is extended to finite temperature in Sec. III, where we present results for the behavior of the nucleon mass in the zero-width approximation. However, at low temperature we expect the nucleon to acquire a temperature-dependent width from $N\to\pi\Delta$ and $\pi N\to\Delta$ processes in the heat bath. These effects are discussed in Sec. IV and incorporated in the QCD sum-rule analysis. Our results are compared to the recent results discussed by Leutwyler and Smilga [4] using finite-temperature chiral perturbation analysis and also a virial expansion. Our conclusions are summarized in Sec. V.

II. THE NUCLEON IN THE VACUUM

The QCD sum-rule approach [7] to mesons has been extended to nucleons by Ioffe [8]. We begin our discussion by summarizing the construction in the vacuum. To probe the nucleon channel in the context of the QCD sum rules, we use the Ioffe current:

$$\eta_N(x)=\epsilon^{abc}[u^a(x)C\gamma_\mu u^b(x)][\gamma_5\gamma_\mu d^c(x)] .$$

Other choices are also possible. We will not pursue them in this work. In the vacuum the nucleon-nucleon correlation function in momentum space reads

$$\Pi(q)=i\int d^4x\, e^{iq\cdot x}\langle T[\eta_N(x)\bar\eta_N(0)]\rangle . \tag{2.1}$$

Covariance implies two invariant structure functions

$$\Pi(q^2)=\not q\,\Pi_1(q^2)+\Pi_2(q^2) . \tag{2.2}$$

For large external momenta (short distances) we can use the operator-product expansion (OPE) to separate perturbative short-distance fluctuations in the form of Wilson coefficients, from nonperturbative long-distance fluctuations in the form of matrix elements. If μ is the typical renormalization scale then

$$\Pi_1(q^2)=\mathcal{C}_1(q^2,\mu^2)1 + \mathcal{C}_{(\bar qq)^2}(q^2,\mu^2)\langle\bar qq(0,\mu^2)\rangle^2+\cdots , \tag{2.3}$$

$$\Pi_2(q^2)=\mathcal{C}_{\bar qq}(q^2,\mu^2)\langle\bar qq(0,\mu^2)\rangle+\cdots . \tag{2.4}$$

Here the $\mathcal{C}$'s stand for the pertinent Wilson coefficients evaluated at fixed Euclidean momentum q^2 at the renormalization point μ. The matrix elements depend in principle on the renormalization point μ. In the QCD sum-rule approach, the expansion is restricted to the lowest-dimensional operators for an optimal choice of

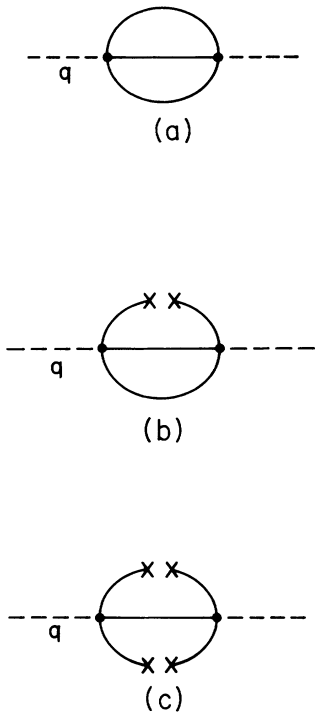

FIG. 1. (a) Leading perturbative contribution in the OPE: coefficient $\mathcal{C}_1$, (b) contribution of the quark condensate $\mathcal{C}_{\bar{q}q}$, (c) contribution of the square condensate $\mathcal{C}_{(\bar{q}q)^2}$.

$\mu \sim 4-5\Lambda$. This will be understood throughout.

For simplicity, we will ignore altogether the effects of gluon condensates such as $\langle G^2 \rangle$ and $\langle G^4 \rangle$ as their effects are known to be small in the nucleon channel [9]. We will also ignore the effects of the mixed operator $\langle \bar{q}(\lambda^a/2)G^a_{\mu\nu}\sigma^{\mu\nu}q \rangle$ as it enters at the same level as the single quark condensate, and its value is usually tied to the latter. In the conventional approach, the inclusion of mixed condensates affects the nucleon mass by about 10% [8]. We expect these effects to be even weaker at finite temperature because of the melting of the vacuum condensates.

The Wilson coefficients can be calculated in perturbation theory at high Euclidean momenta $-q^2=Q^2 \to \infty$ as shown in Fig. 1. For the Ioffe current

$$\Pi_1(Q^2) = -\frac{Q^4}{64\pi^4}\ln\left[\frac{Q^2}{\mu^2}\right] + \frac{2}{3}\langle \bar{q}q \rangle^2 \frac{1}{Q^2} , \tag{2.5}$$

$$\Pi_2(Q^2) = -\frac{Q^2}{4\pi^2}\langle \bar{q}q \rangle \ln\left[\frac{Q^2}{\mu^2}\right] . \tag{2.6}$$

Analyticity implies that each structure function satisfies the (unsubtracted [1]) sum rule

$$\Pi_{1,2}(Q^2) = \frac{1}{\pi}\int_0^\infty \frac{\mathrm{Im}\Pi_{1,2}(s)}{s+Q^2} ds . \tag{2.7}$$

[1]The subtractions drop after Borel transformations [7] and will be ignored.

The imaginary part in (2.7) is not calculable in perturbation theory. In the zero-width approximation, it can be saturated by the nucleon pole term

$$\mathrm{Im}\Pi(q^2) = \lambda_N^2(\not{q}+m_N)\pi\delta(q^2-m_N^2) , \tag{2.8}$$

where λ_N characterizes the overlap between the nucleon state and the vacuum

$$\langle 0|\eta_N(x)|N(p)\rangle = \lambda_N u(p)e^{-ipx} .$$

Inserting (2.5), (2.6), and (2.8) into (2.7) and taking the Borel transform yields two independent sum rules:

$$\hat{L}_M\Pi_1(Q^2) = \frac{M^4}{32\pi^4} + \frac{2}{3}\frac{\langle \bar{q}q \rangle^2}{M^2} = \lambda_N^2 \frac{1}{M^2} e^{-m_N^2/M^2} , \tag{2.9}$$

$$\hat{L}_M\Pi_2(Q^2) = -\frac{M^2}{4\pi^2}\langle \bar{q}q \rangle = \lambda_N^2 \frac{m_N}{M^2} e^{-m_N^2/M^2} , \tag{2.10}$$

where $\hat{L}_M$ is short for the Borel transform (see Appendix B and Ref. [7] for more details), and M the Borel mass. The nucleon mass follows from taking the ratio of (2.9) and (2.10):

$$m_N = \frac{2aM^4}{M^6 + \frac{4}{3}a^2} , \tag{2.11}$$

where $a=-(2\pi)^2\langle \bar{q}q \rangle$. For a Borel mass $M \sim m_N$, it follows that $m_N \sim (2a)^{1/3} \sim 1$ GeV for a condensate $\langle \bar{q}q \rangle \sim (-225\ \mathrm{MeV})^3$.

While the above arguments are schematic they capture the essence of the QCD sum-rule approach to the nucleon in the vacuum. For a more complete and refined analysis, we refer the interested reader to the original literature [8].

III. THE NUCLEON AT FINITE TEMPERATURE

The extension of the QCD sum-rule approach to finite temperature has first been discussed by Bochkarev and Shaposhnikov [10] and was recently reinvestigated by us with special emphasis on the ρ-meson channel [5]. Here we extend the discussion to the nucleon channel. For a complete discussion, the interested reader is referred to Ref. [5].

In the real-time approach to finite-temperature field theory the fermion propagator acquires a temperature-dependent piece

$$iS(p) = \frac{i}{\not{p}-m} - 2\pi(\not{p}+m)\delta(p^2-m^2)n_F(p) , \tag{3.1}$$

where $n_F(p)$ is the Fermi distribution function ($\beta=1/T$):

$$n_F(p) = \frac{1}{e^{\beta|p_0|}-1} . \tag{3.2}$$

This alteration of the zero-temperature Feynman rules will suffice for our purposes, since there are no internal vertices in the graphs of Fig. 1. (In graphs with internal vertices, care must be taken to include so-called "ghost vertices," to cancel the occurrence of pinch singularities, see, e.g., [11].)

In the imaginary-time approach, temperature is introduced by restricting integrations along the Euclidean time axis to a finite interval of extent $i\beta = i/T$, while integration over energies is replaced by finite sums over the discrete Matsubara frequencies.[2] Both approaches lead ultimately to the same results but differ in calculational complexity. In order to have a check on the results it is often useful to use both methods, as we have done in the subsequent calculations.

To set up the sum rules for the nucleons at finite temperature, we need both the temperature dependence of the Wilson coefficients and that of the condensates. The temperature dependence of the condensates (the quark condensate in this case) is entirely nonperturbative and cannot be estimated perturbatively. The origin of this temperature dependence lies in the implicit temperature dependence of the nonperturbative ground state through the quark-gluon coupling constant $g(\Lambda, T)$ via the renormalization group (Λ is the renormalization scale). The temperature dependence of the Wilson coefficients however *is* perturbative, and can be obtained via the standard methods mentioned above.

Starting from the nucleon correlator at finite temperature in the Matsubara approach,

$$\Pi(q^2) = i \int_0^{i\beta} dx_0 \int d^3x \, e^{iqx} \langle 0 | T_\tau [\eta_N(x) \bar{\eta}_N(0)] | 0 \rangle \ , \tag{3.3}$$

or from the retarded one in the Gibbs approach, we can extract the lowest-order contributions to the OPE as shown in Fig. 1. The evaluation of the contribution of Fig. 1(a) is straightforward but tedious. For a nucleon at rest in the heat bath ($\mathbf{q} \to \mathbf{0}$) we have ($\omega_\pm = \omega \pm \omega'$)

$$\begin{aligned}
\Pi^{1(a)} = \gamma_0 q_0 \Bigg\{ & -\frac{(-q_0^2)^2}{64\pi^4} \ln\left[-\frac{q_0^2}{\mu^2}\right] - \frac{7}{12} T^4 \ln\left[-\frac{q_0^2}{\mu^2}\right] - \frac{5}{\pi^4} \int_0^\infty \omega^3 d\omega \, n_F(\omega) \ln\left[1 - \frac{4\omega^2}{q_0^2}\right] \\
& - \frac{3q_0}{\pi^4} \int_0^\infty \omega^2 d\omega \, n_F(\omega) \ln \frac{\omega + q_0/2}{-\omega + q_0/2} \\
& + \frac{6}{\pi^4} \int_0^\infty d\omega d\omega' n_F(\omega) n_F(\omega') \\
& \times \Bigg[\left[\omega^2 + \omega'^2 + \frac{q_0^2}{4}\right] \ln \frac{1 - 4\omega_-^2/q_0^2}{1 - 4\omega_+^2/q_0^2} + q_0 \omega_- \ln \frac{\omega_- + q_0/2}{-\omega_- + q_0/2} - q_0 \omega_+ \ln \frac{\omega_+ + q_0/2}{-\omega_+ + q_0/2} \\
& + 2\omega q_0 \ln \frac{\omega' + q_0/2}{-\omega' + q_0/2} + 2\omega' q_0 \ln \frac{\omega + q_0/2}{-\omega + q_0/2} \\
& - \omega\omega' \ln[(1 - 4\omega_+^2/q_0^2)(1 - 4\omega_-^2/q_0^2)] + 2\omega\omega' \ln[(1 - 4\omega^2/q_0^2)(1 - 4\omega'^2/q_0^2)] \Bigg] \Bigg\} \ .
\end{aligned} \tag{3.4}$$

The first term in (3.4) corresponds to the vacuum contribution, the second, third, and fourth terms arise by choosing one of the three quarks from the heat bath (hence on shell), a situation reminiscent of Fig. 1(b).[3] These effects arise from perturbative thermal contributions to the quark condensate as shown in Appendix A. They appear in the Wilson coefficients after reordering around the blackbody spectrum. This point was thoroughly discussed by Hansson and one of us in the context of a free massless scalar theory [12]. The fifth term in (3.4) is obtained by taking two out of the three quarks from the heat bath.

The contribution of Fig. 1(b) is given by

$$\begin{aligned}
\Pi^{1(b)} = & \frac{\langle \bar{q} q \rangle}{4\pi^2} q_0^2 \ln\left[-\frac{q_0^2}{\mu^2}\right] \\
& + \frac{4\langle \bar{q} q \rangle}{\pi^2} \int_0^\infty \omega^3 d\omega \frac{n_F(\omega)}{\omega^2 - q_0^2/4} \ .
\end{aligned} \tag{3.5}$$

The contribution of Fig. 1(c) is temperature independent:

$$\Pi^{1(c)} = -\frac{2}{3} \frac{\langle \bar{q} q \rangle^2}{q_0^2} \ . \tag{3.6}$$

Before proceeding further, we would like to make some important remarks. The use of the OPE in the context of the sum-rule approach is based on the premise that the power corrections from higher-dimensional operators are small compared to the perturbative contribution. In this respect higher-dimensional operators are ignored at the renormalization point μ. At finite temperature T stands for a new scale and power corrections of the form T^2/Q^2, T^4/Q^4, ... (with $Q^2 = -q_0^2$) do arise. They arise from

[2]For a review of these techniques, see Ref. [11].

[3]The ultraviolet divergence in the second term of (3.4) has been removed by a zero-temperature renormalization of the pertinent current. A similar remark applies to the lowest-order perturbative temperature contribution to Fig. 1(b) (see Appendix A).

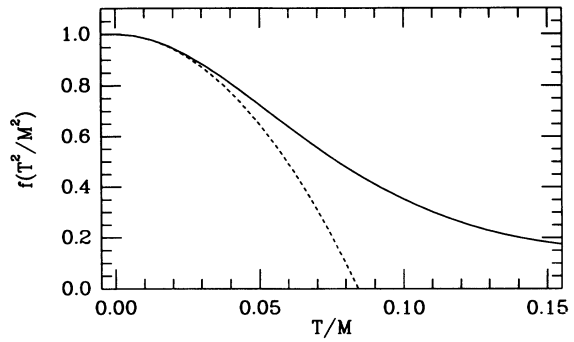

FIG. 2. The function $f(T^2/M^2)$ that multiplies the perturbative temperature contribution. Solid line: summing *all* orders, dashed line: expanding to order T^2/M^2.

the blackbody part of the higher-dimensional operators as noted earlier, and have been resummed to all orders in the computation of the Wilson coefficients above. This resummation is *a priori* inconsistent since higher-dimensional operators have been ignored. We think however, that the effects of temperature for the perturbative (blackbody) contribution, and the nonperturbative (soft) contribution, work in opposite directions: they enhance the former and reduce the latter. What is clear from our present estimates is that the blackbody effects are only small at very low temperatures. To stress this point and provide a fair discussion, we have in addition to using the full Wilson coefficients, expanded these coefficients to order T^6/Q^2 (the same order in $1/Q^2$ that has been kept in the OPE at zero temperature) neglecting the rest. Figure 2 compares the expanded and the full dependence of the function $f(T^2/M^2)$ which appears in the sum rule below (and in Appendix B). It is apparent from this figure that the temperature expansion is reliable for low temperatures (about 50 MeV). At higher temperatures all our results have to be taken with a grain of salt, assuming that the nonperturbative zero- and finite-temperature content of higher-order condensates is small. The latter is usually assumed in the conventional sum-rule analysis.

Having said this we now proceed to write down the QCD sum rules in the nucleon channel at finite temperature. They follow from the dispersion relations for each structure function, in the same manner as Eq. (2.7). Note however that these relations now hold in the limit $\mathbf{Q}\to 0$ (source at rest) because of the special frame provided by the heat bath. This limit will be understood throughout. For Π_1 we obtain, after Borel transformation,[4]

$$M^6+\frac{4}{3}a^2+\frac{56}{3}\pi^4T^4M^2f\left[\frac{T^2}{M^2}\right]=2(2\pi)^4\lambda_N^2e^{-m_N^2/M^2}. \tag{3.7}$$

The third term on the left-hand side (LHS) summarizes the effects of temperature on the perturbative contribution to the correlator, Fig. 1(a). The explicit form of the function $f(T^2/M^2)$ is given in Appendix B and plotted in Fig. 2. For Π_2, and again after Borel transformation, the QCD sum rule reads

$$aM^4\left[1-\frac{64}{M^2}\int\omega^3d\omega\, n_F(\omega)e^{-4\omega^2/M^2}\right]=(2\pi)^4\lambda_N^2m_Ne^{-m_N^2/M^2}. \tag{3.8}$$

Taking the ratio of (3.7) and (3.8) we obtain

$$m_N=\frac{2aM^2\left[1-64\frac{T^4}{M^4}\int\omega^3d\omega\, n_F(\omega)e^{-4\omega^2T^2/M^2}\right]}{M^4+\frac{4}{3}a^2/M^2+\frac{56}{3}\pi^4T^4f(T^2/M^2)}. \tag{3.9}$$

Note that neither the possibility of a finite-temperature width (zero-width approximation) nor threshold effects are included in the derivation of (3.9). These two issues will be discussed in the next section.

Equation (3.9) gives an estimate of the nucleon mass as a function of the Borel parameter M and the temperature. The QCD sum-rule prediction is obtained by finding the value of M for which $\partial m_N(M)/\partial M=0$. This leads to the results in Figs. 3(a) and 3(b) (solid lines) for the following two cases.

(i) The quark condensate does not vary between $T=0$ and $T=T_c$. This is the extreme case that might be real-

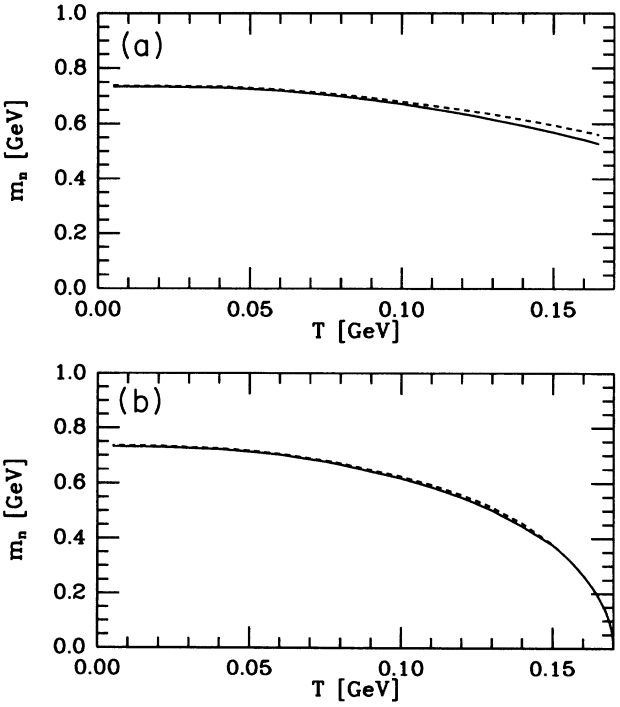

FIG. 3. (a) Nucleon mass vs temperature for a constant quark condensate. Solid line: without continuum corrections, dashed line: including the $\pi\Delta$ continuum. (b) Same as (a) but with a condensate dropping as $\sqrt{1-(T/T_c)^2}$, with $T_c=170$ MeV.

[4]Formulas that are needed to perform this transformation are given in Appendix C.

ized in a first-order phase transition. The result is the solid curve in Fig. 3(a).

(ii) The quark condensate varies with temperature as

$$\langle \bar{q}q \rangle_T = \langle \bar{q}q \rangle_0 \left[1 - \left[\frac{T}{T_c} \right]^2 \right]^{1/2} , \tag{3.10}$$

where we arbitrarily chose $T_c = 170$ MeV. This case seems likely in the event the phase transition turns out to be second order. The result is the solid line in Fig. 3(b).

As is apparent from these figures, because of the soft temperature dependence of the nucleon mass in the case the condensate is kept constant, the behavior of m_N as a function of T is mainly dictated by the behavior of the quark condensate. This point was already noted as zero temperature.

IV. THRESHOLD EFFECTS AND BROADENING AT FINITE TEMPERATURE

Our analysis so far has ignored the effects of a continuum in the nucleon channel as well as the possibility of a thermal broadening of the nucleon state. At zero temperature, the short-distance part of the correlator is dominated by the perturbative three-quark diagram Fig. 1(a), the imaginary part of which gives the nucleon continuum as conventionally used [8]. However, it seems unreasonable to expect the three-quark continuum to be important at intermediate momentum transfers of ~ 1.5 GeV. A look at πN dynamics in this region shows that the nucleon correlator is dominated by effects of the Δ resonance, dwarfing other processes, such as elastic πN scattering. As we expect the heat bath below T_c to consist predominantly of pions, we anticipate the prime mechanism for nucleon loss to be the processes depicted in Fig. 4, namely absorption of a pion from the heat bath [Fig. 4(a)] $\pi N \to \Delta$, and the real dissociation process $N \to \pi\Delta$ [Fig. 4(b)]. While the latter process contributes to the continuum at zero and finite temperature, it is the former one which gives the nucleon a finite width at finite temperature. The amplitude for this process vanishes at $T=0$.

To describe $\pi N\Delta$ dynamics at zero and finite temperature, we use an effective interaction that has been used successfully to reproduce the effects of the Δ resonance at low energy in the analysis of πN scattering (see, e.g., Höhler, Jakob, and Strauss [13], and references therein). Note that as we are only interested in the imaginary part of the self-energy, which all the particles are on shell, the interaction is unique:

$$\mathcal{L}_{\rm int} = \frac{g}{m_\pi} \{ \bar{Z}^a_{\mu\alpha} \partial_\mu \pi^a \psi_\alpha + \text{H.c.} \} . \tag{4.1}$$

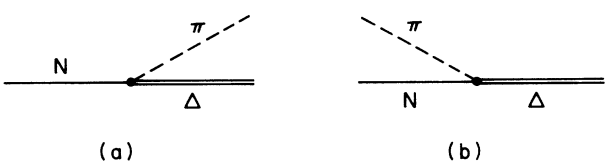

FIG. 4. Processes contributing to nucleon "absorption" in a pionic heat bath: (a) "real" process, (b) "virtual" process.

Here $Z^a_{\mu\alpha}$ is the four-component Rarita-Schwinger field describing the elementary Δ, while π^a is the pion, and ψ_α the nucleon field. The dimensionful coupling g/m_π is normalized in such a way as to reproduce the width of the Δ. With the interaction (4.1) we find

$$\Gamma_\Delta = \frac{1}{12\pi} \frac{g^2}{m_\pi^2} \frac{E_N + m_N}{M_\Delta} |\mathbf{q}_\pi|^3 \tag{4.2}$$

which yields $g^2 \sim 4.68$ for $\Gamma_\Delta = 115$ MeV. In the above expression, E_N is the nucleon energy and $\mathbf{q}_\pi$ the pion momentum in the Δ rest frame. Some properties of the spin-$\frac{3}{2}$ field $Z^a_{\mu\alpha}$ as well as the Δ propagator are listed in Appendix D.

The processes illustrated in Fig. 4 can be incorporated into the correlator by dressing the nucleon propagator with the $\pi\Delta$ self-energy diagram Fig. 5. Using the Δ propagator from Appendix D we find, at zero temperature,

$$\Sigma_{\pi\Delta}(\not p) = -\frac{4}{3} \frac{g^2}{m_\pi^2} \int \frac{d^4k}{(2\pi)^4} \frac{\not p + \not k + M_\Delta}{(p+k)^2 - M_\Delta^2} \times \frac{k^2 - \dfrac{[k\cdot(p+k)]^2}{M_\Delta^2}}{k^2 - m_\pi^2} . \tag{4.3}$$

The dressed nucleon propagator is given by (m_0 is the bare nucleon mass)

$$iS(p) = \frac{i}{\not p - m_0 - \Sigma_{\pi\Delta}(\not p) + i\epsilon} . \tag{4.4}$$

To renormalize, we expand the self-energy (we drop the subscript $\pi\Delta$ and denote the physical nucleon mass by m_N)

$$\Sigma(\not p) = \Sigma(\not p)\big|_{\not p = m_0} + (\not p - m_0) \frac{\partial \Sigma(\not p)}{\partial \not p}\bigg|_{\not p = m_0} + \Sigma_R(\not p) \tag{4.5}$$

and require

$$\Sigma_R(\not p)\big|_{\not p = m_0} = \frac{\partial \Sigma_R}{\partial \not p}\bigg|_{\not p = m_0} = 0 . \tag{4.6}$$

The first contribution in (4.5) renormalizes the nucleon mass while the second contribution renormalizes the propagator itself. Carrying out this procedure for the real part of (4.5) we obtain

$$iS_R(\not p) = \frac{i}{\not p - m_N - i\,\text{Im}\Sigma + i\epsilon} , \tag{4.7}$$

where now the first and second terms of (4.5) have been

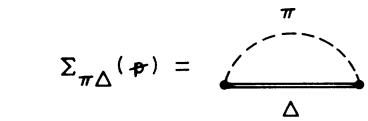

FIG. 5. $\pi\Delta$ self-energy correction to nucleon propagator.

absorbed in mass and wave-function renormalization.[5] This ensures that the pole of the nucleon propagator is at the physical nucleon mass.

The RHS of the QCD sum rules involves the imaginary part of this correlator, as

$$\mathrm{Im}\Pi(q^2)=\lambda_N^2 \mathrm{Im}S_R(q^2) \ . \tag{4.8}$$

From (4.7) it follows that

$$\mathrm{Im}S_R(\not p)=-\frac{\mathrm{Im}\Sigma(\not p)}{(\not p-m_N)^2+(\mathrm{Im}\Sigma)^2} \ . \tag{4.9}$$

The calculation of $\mathrm{Im}\Sigma$ at finite temperature is easiest in the real-time approach, using the finite-temperature Cutkosky rules of Kobes and Semenoff [14]. In the notation of Fig. 6,

$$\mathrm{Im}\Sigma=-\tfrac{1}{2}(\Sigma^{(1)}-\Sigma^{(2)})=-\tfrac{1}{2}(1+e^{-p_0/T})\Sigma^{(2)} \ , \tag{4.10}$$

where $\Sigma^{(1)}$ and $\Sigma^{(2)}$ are defined in Fig. 6. $\Sigma^{(2)}$ is evaluated using the basic scalar bosonic and fermionic on-shell finite-temperature propagators [14]:

$$\Delta_{\pm}(k^2)=2\pi[\theta(\pm k_0)+n_B(k)]\delta(k^2-m^2) \ , \tag{4.11}$$

$$S_{\pm}(p^2)=2\pi[\theta(\pm p_0)-n_F(p)]\delta(p^2-m^2) \ . \tag{4.12}$$

from which it follows that

$$\Sigma^{(2)}=-\frac{4}{3}\frac{g^2}{m_\pi^2}\int\frac{d^4k}{(2\pi)^4}\Delta_-(k^2)\left[k^2-\frac{[k\cdot(p+k)]^2}{M_\Delta^2}\right]\times(\not p+\not k+M_\Delta)S_+[(p+k)^2] \ . \tag{4.13}$$

Neglecting the temperature dependence in the Δ propagator implies $S_-[(p+k)^2]\to 0$ and thus $\Sigma^{(1)}\to 0$. Taking the limit $|\mathbf{p}|\to 0$ we obtain

FIG. 6. Diagrams contributing to the imaginary part of Fig. 5 at finite temperature. The "encircled-vertex" notation is described in [14].

$$\mathrm{Im}\Sigma=(\alpha\not p_0+M_\Delta)\sigma(p_0^2) \tag{4.14}$$

with

$$\sigma(p_0^2)=-\frac{2}{3}\frac{g^2}{m_\pi^2}\theta(p_0)\frac{(t^4-4m_\pi^2p_0^2)^{3/2}}{32\pi M_\Delta^2 p_0^2}\times\left\{\theta(p_0^2-s_+)\left[1+n_B\left[\frac{z}{2}p_0\right]\right]+\theta(s_--p_0^2)n_B\left[-\frac{z}{2}p_0\right]\right\} \tag{4.15}$$

and the definitions

$$t^2=p_0^2-M_\Delta^2+m_\pi^2 \ , \quad z=\frac{t^2}{p_0^2} \ , \tag{4.16}$$

$$\alpha=1-\frac{z}{2} \ , \quad s_\pm=(M_\Delta\pm m_\pi)^2 \ . \tag{4.17}$$

There are two cuts in (4.15). Above s_+, the imaginary part of the self-energy is given by the real process Fig. 4(a). This contribution is multiplied by $(1+n_B)$ and thus is nonvanishing at $T=0$. The virtual process Fig. 4(b) is relevant for $p_0^2<s_-$ and vanishes at $T=0$. Using (4.14) we can now rewrite (4.9) in the form

$$\mathrm{Im}S_R(p)=-\sigma\frac{\not p[\alpha(p_0^2+m_N^2+\mu^2\sigma^2)+2m_NM_\Delta]+M_\Delta(p_0^2+m_N^2-\mu^2\sigma^2)+2m_N\alpha p_0^2}{(p_0^2-m_N^2+\mu^2\sigma^2)^2+4p_0^2\sigma^2(\alpha m_N+M_\Delta)^2} \ , \tag{4.18}$$

where $\mu^2=\alpha^2p_0^2-M_\Delta^2$. This allows us to separate the contributions for the two structure functions Π_1, and Π_2 defined in (2.2), with ($s=p_0^2$)

$$\mathrm{Im}\Pi_1(s)=\lambda_N^2\rho_1(s) \ , \tag{4.19}$$

$$\mathrm{Im}\Pi_2(s)=\lambda_N^2 m_N\rho_2(s) \ , \tag{4.20}$$

where we have defined

$$\rho_1(s)=-\sigma(s)\frac{\alpha(s+m_N^2+\mu^2\sigma^2)+2m_NM_\Delta}{(s-m_N^2+\mu^2\sigma^2)^2+4s\sigma^2(\alpha m_N+M_\Delta)^2} \ , \tag{4.21}$$

$$\rho_2(s)=-\sigma(s)\frac{(M_\Delta/m_N)(s+m_N^2-\mu^2\sigma^2)+2\alpha s}{(s-m_N^2+\mu^2\sigma^2)^2+4s\sigma^2(\alpha m_N+M_\Delta)^2} \ . \tag{4.22}$$

Taking again the ratio of the Borel-transformed structure functions we obtain an expression for the nucleon mass where now the left-hand side of Eq. (3.9) is replaced by

$$\mathrm{RHS}=m_N\frac{\int_0^\infty e^{-s/M^2}\rho_2(s)ds}{\int_0^\infty e^{-s/M^2}\rho_1(s)ds}\equiv m_N Z \ . \tag{4.23}$$

Figure 7(a) shows the behavior of ρ_1 and ρ_2 for a temperature of 100 MeV and a nucleon mass $m_N=0.67$ GeV (as opposed to $m_N=0.73$ GeV at $T=0$; remember that we are not at the moment interested in a quantitative determination of the nucleon mass, but rather in a statement about the qualitative behavior). The region below s_- is dominated by the nucleon resonance with a finite

[5]We neglect here a small momentum-dependent shift of the nucleon mass to $m_N^*=m_N+\mathrm{Re}\Sigma_R(\not p)\sim m_N$. This is certainly a good approximation near the pole.

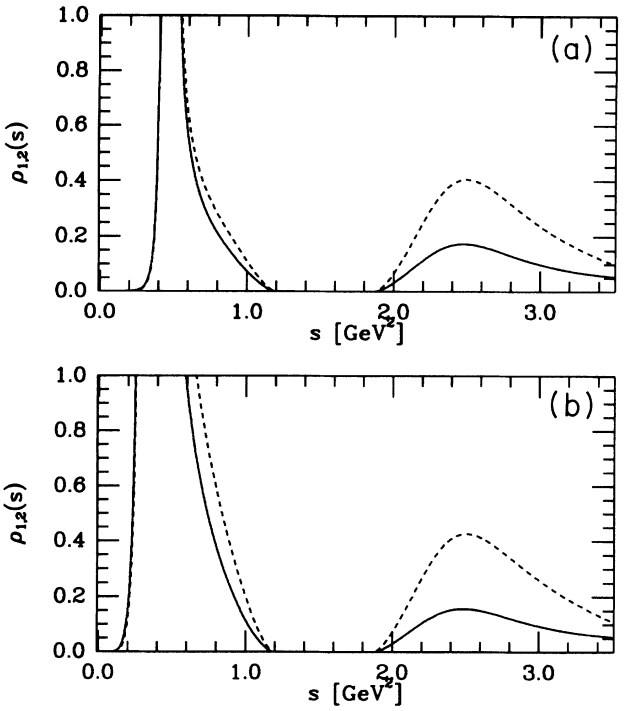

FIG. 7. The structure functions $\rho_1(s)$ (solid line) and $\rho_2(s)$ (dashed line) of the imaginary part of the nucleon correlator, (a) $T=100$ MeV with $m_N=0.67$ GeV, (b) $T=150$ MeV and $m_N=0.58$ GeV.

width (at half maximum) $\Gamma\sim 5$ MeV, while the continuum starts at s_+. Figure 7(b) shows ρ_1 and ρ_2 at the higher temperature $T=150$ MeV. The continuum is almost unchanged, while the width is strongly affected by temperature. This will be discussed in more detail below.

The "correction factor" Z in (4.23) which summarizes the effects of the continuum can be made more transparent by splitting the contributions from the real and virtual processes: the integral over ρ_1 below s_- differs from the integral over a δ function only by at most 2%. Thus, for the calculation of the nucleon *mass*, we can approximate this part of the spectrum by $\pi\delta(s-m_N^2)$. (This is of course exact in the limit $T\to 0$). Hence

$$Z=\frac{1+\frac{1}{\pi}e^{m_N^2/M^2}\int_{s_+}^{\infty}ds\,e^{-s/M^2}\rho_2(s)}{1+\frac{1}{\pi}e^{m_N^2/M^2}\int_{s_+}^{\infty}ds\,e^{-s/M^2}\rho_1(s)}\,. \tag{4.24}$$

As is apparent from Figs. 7(a) and 7(b), the continuum contribution is overshadowed by the resonance, and indeed it turns out that the continuum corrections to the resonance contribution (normalized to 1), are of the order 10^{-3}. For this reason, Z differs from 1 by a fraction to a few % only, depending on the value of the Borel mass. Thus, the $\pi\Delta$ continuum does not appreciably affect the nucleon mass. We have, as an example, plotted the nucleon mass m_N against the Borel mass M for a temperature $T=100$ MeV and a constant quark condensate in Fig. 8. The solid line is the result for the nucleon mass including the Z factor of (4.23) while the dashed line has

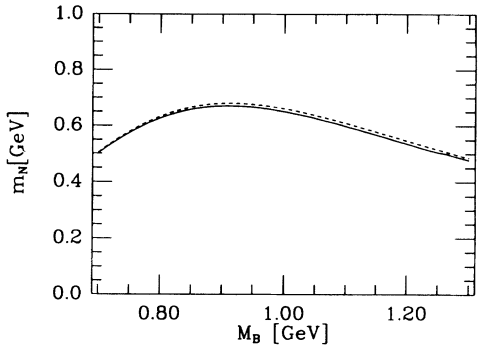

FIG. 8. Nucleon mass m_N vs Borel mass M for a moderate temperature $T=100$ MeV, in the constant-quark-condensate scenario. The solid line is the result of the calculation including the $\pi\Delta$ continuum, the dashed one has $Z=1$, i.e., no continuum.

$Z=1$, i.e., no continuum. The difference between the curves is small, and nearly independent of temperature, as the spectrum above s_+ is remarkably insensitive to temperature [compare Figs. 7(a) and 7(b)]. The result of the calculation including the continuum correction is shown in Figs. 3(a) and 3(b) (dashed lines). We thus conclude that a finite-temperature $\pi\Delta$ continuum does not affect the mass of the nucleon considerably. This is partly at odds with the results reached from a model with a three-quark continuum. Such a model introduces a strong, almost linear, dependence of the nucleon mass on the choice of the continuum threshold s_0. However, the imaginary part of the $3q$ diagram [Fig. 1(a)] has not been calculated at finite temperature (this would correspond to a heat bath of free quarks and gluons), and thus no direct comparisons can be made. We would like to note however that the continuum model developed above, unlike the three-quark one, fixes the threshold unequivocally by the kinematics. The only uncertainty lies in the value of M_Δ at finite temperature (assuming the pion mass to be about constant below T_c). Still, our results seem to be stable against small variations in M_Δ.

We would also like to compare these results with the virial expansion approach of Leutwyler and Smilga [4]. Their approach relies on the measured total πN cross section as an input, which is dominated by the presence of the Δ resonance, to monitor the changes to the nucleon propagator (position of the pole and damping rate). They find a nucleon mass dropping slightly at intermediate temperatures but rising at temperatures $T\sim 150$ MeV, and a nucleon width rising rapidly with temperature for $T>50$ MeV. To make an explicit comparison with our results consider the nucleon width as defined by

$$\gamma_N=-2[\mathrm{Im}S_R(p_0=m_N)]^{-1}\,. \tag{4.25}$$

In the pole region (4.25) can be simplified to

$$\gamma_N=\frac{1}{3\pi}\frac{g^2}{m_\pi^2}\frac{E_N+m_N}{M_\Delta}|\mathbf{q}_\pi|^3 n_B\left[\frac{\omega_\Delta}{T}\right]$$
$$=4\Gamma_\Delta\left[\frac{M_\Delta}{m_N}\right]^3 n_B\left[\frac{\omega_\Delta}{T}\right], \tag{4.26}$$

TABLE I. Width of the nucleon in the nonrelativistic approximation. Γ_1 is the width in the first-order scenario (constant quark condensate), while Γ_2 is the width in the second-order scenario (dropping condensate).

T (MeV)	Γ_1 (MeV)	Γ_2 (MeV)
50	1.3×10^{-2}	0.9×10^{-2}
75	0.8	0.5
100	5.0	2.9
125	16.2	3.62
150	30.0	0.56
170	36.3	0.0

where $\omega_\Delta=(2m_N)^{-1}(M_\Delta^2-m_N^2-m_\pi^2)$, $|\mathbf{q}_\pi|$ is the pion momentum in the nucleon rest frame and Γ_Δ is defined in (4.2). Note that this is the expected result in the Born approximation. Table I summarizes the values for γ_N at various temperatures with mass inputs from the sum-rule approach for both approaches (I and II) as described above. The quoted values for the width by Leutwyler and Smilga [4] are 4–10 larger than ours in the range of temperature where the two approaches are reliable. The discrepancy is due to the fact that in our case the nucleon mass is about 200 MeV below the physical mass at zero temperature (as is the case for all sum-rule calculations) and drops with increasing temperature. In the case considered by Leutwyler and Smilga [4] the nucleon mass is fixed to its zero temperature value for the quoted variations in the width.[6] As a result the pion energy ω_Δ in (4.26) is about a factor of 2 larger in our case. The difference occurs in the exponent, hence the discrepancy.

Overall, however, there is qualitative agreement between the two approaches in the regime where either of them can be trusted. For temperatures larger than $T=150$ MeV where the virial approach is known to break down and the QCD sum-rule approach appears to be unreliable due to the neglect of higher-order condensates, the approaches differ.

V. CONCLUSIONS AND PROSPECTS

We have investigated finite-temperature QCD sum rules below T_c in the nucleon channel in an attempt to gain some understanding about the qualitative behavior of the nucleon parameters at moderate temperatures.

While we did not strive to reproduce the zero-temperature parameters, we included what we believe are important ingredients in a finite-temperature analysis. Furthermore we introduced a continuum model which seems more appropriate for the intermediate-energy range probed here, as well as more suited to the physical situation at hand: the pionic heat bath. The results we obtained seem to indicate that the nucleon mass is mainly governed by the finite-temperature behavior of the quark condensate, a feature shared by the simple estimate of Brown [15]. As the condensate disappears smoothly with chiral-symmetry restoration (as suggested by lattice gauge theory and effective model calculations), so does the nucleon mass.

The limitations of the present approach are several. Concerning the left-hand side of the sum rule [Eqs. (2.5) and (2.6), viz. (3.7) and (3.8)] it is clear that higher-order condensates may become increasingly important near T_c in a second-order scenario (much less in a first-order scenario). Moreover the possibility of spontaneous breaking of global color above T_c may provide new condensates [12] and hence possibly a nonvanishing nucleon mass even above the critical temperature (here understood as a chiral-symmetry-restoring temperature). Finite-temperature radiative corrections to the Wilson coefficients have been ignored, much like at zero temperature. Because of screening effects in the charge, we expect this assumption to have a better justification at finite temperature. The parametrization of the right-hand side of (2.7) in the timelike regime may be improved by going beyond the narrow-width approximation for the Δ, as implied in (4.19) and (4.20). However, at temperatures around $T\sim150$ MeV not only pions, but also the heavier vector mesons play a role. While all these points should be addressed, we believe, however, that the present calculation provides qualitative insight into the thermal effects on the nucleon state borrowing on QCD dynamics.

ACKNOWLEDGMENTS

One of us (C.A.) would like to thank Gerry Brown and Wolfram Weise for discussions. This work was supported in part by the U.S. Department of Energy under Grant No. DE-FG02-88ER40388.

APPENDIX A

In this appendix we shall show in detail how temperature-dependent pieces of the perturbative Wilson coefficient arise as the perturbative temperature contributions from condensates appearing in the OPE. This point has been discussed previously in Ref. [12]. The conventional OPE expansion does not refer to temperature effects explicitly. Temperature enters via the vacuum expectation values of the pertinent operators. However, by reordering the operators in the heat bath, the leading blackbody effects in the matrix elements can be reshuffled into the Wilson coefficients. The purpose of this appendix is to show that the reshuffling in real time amounts to calculating the Wilson coefficients using the standard Matsubara formalism as used above.

Consider the lowest-order temperature contribution to Fig. 1(b) using the Gibbs average. The baryon correlator is (repeated indices are summed over, C is the charge-conjugation matrix)

$$\Pi_{\rho\rho'}=i\epsilon^{abc}\epsilon^{def}(C\gamma_\mu)_{\alpha\beta}(\gamma_\mu\gamma_5)_{\rho\sigma}(\gamma_\nu\gamma_5)_{\sigma'\rho'}(\gamma_\nu C)_{\alpha'\beta'}e^{iqx}$$
$$\times\langle\langle\, T{:}u_\alpha^a(x)u_\beta^b(x)d_\sigma^c(x){::}\bar{d}_{\sigma'}^d(0)\bar{u}_{\alpha'}^e(0)\bar{u}_{\beta'}^f(0){:}\,\rangle\rangle\ , \tag{A1}$$

[6] In the narrow resonance approximation, our expression for the nucleon width is identical to theirs up to a kinematical factor of M_Δ/m_N.

where

$$\langle\langle \mathcal{O} \rangle\rangle = \sum_n \langle n|\mathcal{O}|n\rangle e^{-\omega_n/T} \tag{A2}$$

with the summation over a complete set of physical states. The repeated use of Wick's theorem in (A1) leads to various pair contractions. We shall focus on the term involving one uncontracted pair which can be expanded:

$$\begin{aligned}\langle\langle :u^a_\alpha(x)\bar{u}^e_{\alpha'}(0):\rangle\rangle = &-\langle\langle \bar{u}u \rangle\rangle \frac{\delta^{ae}\delta^{\alpha\alpha'}}{12} \\ &+x_\mu \langle\langle \partial_\mu u^a_\alpha(0)\bar{u}^e_{\alpha'}(0)\rangle\rangle \\ &+\tfrac{1}{2}x_\mu x_\nu \langle\langle \partial_\mu\partial_\nu u^a_\alpha(0)\bar{u}^e_{\alpha'}(0)\rangle\rangle \\ &+\cdots . \end{aligned} \tag{A3}$$

To carry out the thermal averages we expand the quark fields into normal modes and use

$$\langle\langle b_i^{\dagger e}(k)b^a_j(k')\rangle\rangle = \delta^{ea}\delta^{ij}(2\pi)^3\frac{k_0}{m}\delta(\mathbf{k}-\mathbf{k}')n_F(k_0) \tag{A4}$$

and similarly for the d and $d^\dagger$ operators. It is then easy to show that, e.g.,

$$x_\mu \langle\langle \bar{u}^e_{\alpha'}(0)\partial_\mu u^a_\alpha(0)\rangle\rangle = -ix_\mu \int \frac{d^3k}{(2\pi)^3}\frac{n_F(k_0)}{k_0}k_\mu \not{k} . \tag{A5}$$

Note that the thermal average of operators with an even number of derivatives is proportional to the quark mass and thus vanishes in the chiral limit. Substituting (A5) into that piece of the nucleon correlator that is proportional to the quark condensate, we obtain the expression for $\Pi^{\bar{q}q}$ given below. Note that the calculation is easiest in the coordinate representation, where the fermion propagator may be written (again in the chiral limit) as

$$S(x) = -\frac{1}{2\pi^2}\frac{\gamma\cdot x}{x^4} . \tag{A6}$$

Thus

$$\Pi^{\bar{q}q}(q) = \frac{48}{\pi^4}\int \frac{d^3k}{(2\pi)^3}\frac{n_F(k_0)}{k_0}\int d^4x\, e^{iqx}\frac{x\cdot k}{x^8} \times [x^2\not{k} + 2(x\cdot\gamma)(x\cdot k)] . \tag{A7}$$

The final result follows using some formulas for Fourier transforms which are listed here for convenience (in dimensional regularization with $D=4-2\epsilon$):

$$\int \frac{d^Dx}{(x^2)^n}x_\mu e^{iqx} = \frac{(-1)^{n+1}}{2^{2n}}32\pi^2\left[\frac{-q^2}{4\pi}\right]^\epsilon \frac{\Gamma(3-n-\epsilon)}{\Gamma(n)}(-q^2)^{n-3}q_\mu , \tag{A8}$$

$$\int \frac{d^Dx}{(x^2)^n}x_\mu x_\nu e^{iqx} = \frac{(-i)(-1)^{n+1}}{2^{2n}}32\pi^2\left[\frac{-q^2}{4\pi}\right]^\epsilon \left[\frac{\Gamma(3-n-\epsilon)}{\Gamma(n)}g_{\mu\nu} - 2\frac{q_\mu q_\nu}{q^2}\frac{\Gamma(4-n-\epsilon)}{\Gamma(n)}\right](-q^2)^{n-3} , \tag{A9}$$

$$\begin{aligned}\int \frac{d^Dx}{(x^2)^n}x_\mu x_\nu x_\rho e^{iqx} = &\frac{(-1)^n}{2^{2n-2}}16\pi^2\left[\frac{-q^2}{4\pi}\right]^\epsilon \\ &\times\left[(g_{\mu\nu}q_\rho + g_{\mu\rho}q_\nu + g_{\nu\rho}q_\mu)\frac{\Gamma(4-n-\epsilon)}{\Gamma(n)} - 2\frac{q_\mu q_\nu q_\rho}{q^2}\frac{\Gamma(5-n-\epsilon)}{\Gamma(n)}\right](-q^2)^{n-4} .\end{aligned} \tag{A10}$$

In the limit $\mathbf{q}\to 0$ we obtain[7]

$$\Pi^{\bar{q}q}(q) = -10\frac{\gamma_0 q_0}{\pi^4}\frac{7\pi^4}{120}T^4\left[\frac{1}{\epsilon} + \ln\left[-\frac{q_0^2}{\mu^2}\right] + O(1)\right] . \tag{A11}$$

After removing the $1/\epsilon$ pole by properly renormalizing the currents appearing in the baryon correlator this is precisely the second term of (3.4) obtained using the Matsubara formalism for the Wilson coefficient of Fig. 1(a). Higher orders may be obtained by calculating further pieces in the expansion (A3). In the chiral limit the next term stems from the fourth term in the expansion, which reads $(1/3!)x_\mu x_\nu x_\rho\langle\langle \partial_\mu\partial_\nu\partial_\rho u^a_\alpha(0)\bar{u}^e_{\alpha'}(0)\rangle\rangle$. Its contribution is finite and of order $O(T^6/Q^2)$.

APPENDIX B

Here we give the explicit form of the function $f(T^2/M^2)$ which enters in the sum rule for Π_1, Eq. (3.7). We find, with $x_\pm = x \pm x'$,

[7]The terms of $O(1)$ in this expression vanish after Borel transformation.

$$f\left[\frac{T^2}{M^2}\right]=1-\frac{72}{7\pi^4}\left\{\int dx\,dx' n_F(x)n_F(x')\left[e^{-4x_-^2T^2/M^2}\left[4x_-^2+\frac{M^2}{4T^2}+xx'\right]-e^{-4x_+^2T^2/M^2}\left[4x_+^2+\frac{M^2}{4T^2}-xx'\right]\right.\right.$$
$$\left.+x_+\frac{M}{T}\mathrm{erf}\left[2x_+\frac{T}{M}\right]-x_-\frac{M}{T}\mathrm{erf}\left[2x_-\frac{T}{M}\right]\right]$$
$$-\int x\,dx\,n_F(x)\left[e^{-4x^2T^2/M^2}-\frac{M}{2xT}\mathrm{erf}\left[2x\frac{T}{M}\right]\right](x^2-\tfrac{1}{2}\pi^2)$$
$$\left.+\tfrac{5}{6}\int x\,dx\,n_F(x)(1-e^{-4x^2T^2/M^2})(x^2-\tfrac{2}{5}\pi^2)\right\}. \tag{B1}$$

In the above we used $n_F(x)=(1+e^x)^{-1}$. The function $\mathrm{erf}(x)$ is the error integral:[8]

$$\mathrm{erf}(x)=\int_0^x e^{-t^2}dt\ . \tag{B2}$$

The low-temperature expansion of $f(T^2/M^2)$ is found to be

$$f\left[\frac{T^2}{M^2}\right]=1-\frac{2096}{147}\pi^2\frac{T^2}{M^2}+O\left[\frac{T^4}{M^4}\right]. \tag{B3}$$

APPENDIX C

This appendix contains some useful relations involving Borel transforms. The Borel transformation L_M used throughout the paper is defined as

$$\hat{L}_M=\lim_{\substack{Q^2,n\to\infty\\ Q^2/n=M^2}}\frac{1}{(n-1)!}[Q^2]^n\left[-\frac{\partial}{\partial Q^2}\right]^n. \tag{C1}$$

Some useful transforms read

$$\hat{L}_M\frac{1}{(s+Q^2)^m}=\frac{1}{\Gamma(m)}\frac{1}{M^{2m}}e^{-s/M^2}, \tag{C2}$$

$$\hat{L}_M f(Q^2)=-M^2\hat{L}_M\frac{\partial f(Q^2)}{\partial Q^2}\ . \tag{C3}$$

The last relation implies

$$\hat{L}_M Q^{2m}\ln Q^2=\Gamma(m+1)(-1)^{m+1}M^{2m}\ . \tag{C4}$$

Also

$$\hat{L}_M\ln(1+4\omega^2/Q^2)=1-e^{-4\omega^2/M^2}, \tag{C5}$$

$$\hat{L}_M Q^2\ln(\omega^2+Q^2/4)=M^2e^{-4\omega^2/M^2}(1+4\omega^2/M^2) \tag{C6}$$

and finally

$$\hat{L}_M\omega Q\arctan(2\omega/Q)=\omega^2e^{-4\omega^2/M^2}-\frac{\omega M}{2}\mathrm{erf}(2\omega/M), \tag{C7}$$

where $\mathrm{erf}(x)$ is the error function defined in Appendix B.

[8]Usually the normalized error function is quoted $\mathrm{Erf}(x)=\frac{2}{\sqrt{\pi}}\int_0^x e^{-t^2}dt$.

APPENDIX D

Here we list some properties of the Rarita-Schwinger field $Z^a_{\mu\alpha}$ and give the $I=J=3/2$ propagator. A free spin-$\frac{3}{2}$, isospin-$\frac{3}{2}$ particle can be described by the quantity $Z^a_{\mu\alpha}(x)$, which transforms as a four-vector on the μ index, and as a spinor on the α index. Its wave function can be written as a product of a spin wave function and an isospin wave function:

$$Z^{aM_JM_T}_{\mu\alpha}(k)=\Psi^{M_J}_{\mu\alpha}(k)\Psi^a_{M_T}\ . \tag{D1}$$

$\Psi_{\mu\alpha(k)}$ is a solution to the free-field Dirac equation

$$(\not{k}-M_\Delta)\Psi^{M_J}_{\mu\alpha}(k)=0\ . \tag{D2}$$

In order to restrict this 8-component function to the 4 physical ones, we have to impose subsidiary conditions. They are usually taken to be

$$\gamma_\mu\Psi^{M_J}_{\mu\alpha}=0\ ,\quad k_\mu\Psi^{M_J}_{\mu\alpha}=0\ . \tag{D3}$$

One can then show that

$$\sum_{M_J}\Psi^{M_J}_{\mu\alpha}\Psi^{M_J}_{\nu\beta}=\frac{\not{k}+M_\Delta}{2M_\Delta}\left[g_{\mu\nu}-\frac{1}{3}\gamma_\mu\gamma_\nu-\frac{2k_\mu k_\nu}{M_\Delta^2}+\frac{k_\mu\gamma_\nu-k_\nu\gamma_\mu}{3M_\Delta}\right]_{\alpha\beta}$$
$$\equiv\frac{\not{k}+M_\Delta}{2M_\Delta}G^{\alpha\beta}_{\mu\nu}\ . \tag{D4}$$

The isospin wave function $\Phi^a_{M_T}$ is conveniently written as a Clebsch-Gordan product of a polarization three-vector t and a spinor χ, which are coupled to a $T=3/2$ object:

$$\Phi^1_{M_T}=\sum_{m_t,l}(\tfrac{3}{2}M_T|1l\tfrac{1}{2}m_t)t^a_l\chi_{m_t}\ . \tag{D5}$$

Defining

$$T^a_{M_Tm_t}=\sum_l(\tfrac{3}{2}M_T|1l\tfrac{1}{2}m_t)t^a_l \tag{D6}$$

we can write Φ explicitly as

$$\Phi=\left[\begin{pmatrix} T^{1}_{M_T(1/2)} \\ T^{1}_{M_T(-1/2)} \end{pmatrix}, \begin{pmatrix} T^{0}_{M_T(1/2)} \\ T^{0}_{M_T(-1/2)} \end{pmatrix}, \begin{pmatrix} T^{-1}_{M_T(1/2)} \\ T^{-1}_{M_T(-1/2)} \end{pmatrix}\right] . \quad \text{(D7)}$$

To reduce those six components to four, we again impose a subsidiary condition

$$\tau\cdot\Phi_{M_T}=0 , \quad \text{(D8)}$$

which allows us to calculate the isospin sum

$$\sum_{M_T}\Phi^{a}_{M_T}\Phi^{\dagger b}_{M_T}=\delta^{ab}-\tfrac{1}{3}\tau^{a}\tau^{b} . \quad \text{(D9)}$$

The spin and isospin sums (D4) and (D8) allow us to construct the Δ propagator:

$$\langle 0|TZ^{a}_{\mu\alpha}(x)\bar{Z}^{b}_{\nu\beta}(y)|0\rangle = i\int\frac{d^4k}{(2\pi)^4}e^{-ik(x-y)}\frac{\not{k}+M_\Delta}{k^2-M^2_\Delta+i\epsilon} \times G^{\alpha\beta}_{\mu\nu}(\delta^{ab}-\tfrac{1}{3}\tau^{a}\tau^{b}) \quad \text{(D10)}$$

with $G_{\mu\nu}$ defined in (D4).

[1] *Lattice '90,* Proceedings of the International Conference, Tallahassee, Florida, 1990, edited by U. M. Heller, A. D. Kennedy, and S. Sanielevici [Nucl. Phys. B (Proc. Suppl.) **20** (1991)].

[2] V. L. Eletsky, Phys. Lett. **B 245**, 229 (1990).

[3] M. Dey, V. L. Eletsky, and B. L. Ioffe, Phys. Lett. **B 252**, 620 (1990).

[4] H. Leutwyler and A. V. Smilga, Nucl. Phys. **B342**, 302 (1990).

[5] C. Adami, T. Hatsuda, and I. Zahed, Phys. Rev. **D 43**, 921 (1991).

[6] G. M. Fuller, G. J. Mathews, and C. R. Alcock, Phys. Rev. **D 37**, 1380 (1988).

[7] M. A. Shifman, A. I. Vainshtein, and V. I. Zakharov, Nucl. Phys. **B147**, 385 (1979); **B147**, 448 (1979).

[8] B. L. Ioffe, Nucl. Phys. **B188**, 317 (1981).

[9] A. V. Smilga, Yad. Fiz. **35**, 473 (1982) [Sov. J. Nucl. Phys. **35**, 271 (1982)].

[10] A. I. Bochkarev and M. E. Shaposhnikov, Nucl. Phys. **B268**, 220 (1986).

[11] N. P. Landsman and Ch. G. van Weert, Phys. Rep. **145**, 141 (1987).

[12] T. H. Hansson and I. Zahed, SUNY at Stony Brook Report No. NTG-90-22, 1990 (unpublished).

[13] G. Höhler, H. P. Jakob, and R. Strauss, Nucl. Phys. **B39**, 237 (1972).

[14] R. L. Kobes and G. Semenoff, Nucl. Phys. **B272**, 329 (1986).

[15] G. E. Brown, Nucl. Phys. **A522**, 397c (1991).